iJRASET
International Journal For Research in Applied Science and Engineering Technology

INTERNATIONAL JOURNAL FOR RESEARCH

IN APPLIED SCIENCE & ENGINEERING TECHNOLOGY

Volume: 4 **Issue:** IV **Month of publication:** April 2016

DOI:

www.ijraset.com

Call: 08813907089 | E-mail ID: ijraset@gmail.com

Volume 4 Issue IV, April 2016
ISSN: 2321-9653
International Journal for Research in Applied Science & Engineering Technology (IJRASET)

Design of Endplate to Improve the Rate of Pressure Distribution in Fuel Cell

K.Kamalakannan[1], S.Bhuvanesh[2], A.karthikeyan[3], K.Ilanthazhuthi[4]
[1,2,3,4]*Department of Mechanical Engineering, IFET college of Engineering ,Villupuram.*

Abstract: ***A proper stacking design and cell assembly are important to the performance of fuel cells. The cell assembly will affect the contact behaviour of the bipolar plates with the membrane electrode assembly (MEA). Not enough assembly pressure may lead to leakage of fuels, high contact resistance and malfunctioning of the cells. Too much pressure, on the other hand, may result in damage to the gas diffusion layer or MEA. The stacking design may affect the pressure distribution within the fuel cell stack and thus the interfacial contact resistance. Uneven distribution of the contact pressure will result in hot spots which may have a detrimental effect on fuel cell life. In this study, finite element analysis (FEA) procedures were established for a PEM single cell with point stack assembly method.***

The mechanical properties and geometrical dimensions of all the fuel cell components, such as bipolar plates, membrane, gas diffusion layer and end plates were collected for accurate simulation. From the compliance as well as the pressure distribution of the ordinary endplate fuel cell was calculated. In order to verify the results of the analysis, experimental tests, with a pressure film inserted between the bipolar plates and we were conducted simulation to establish the actual pressure distribution. Color variations of the pressure film could be calibrated to obtain pressure distribution. Compliance of the gas diffusion layer was also measured with the topological optimization of the endplate. The analysis procedures for the fuel cell stacking assembly were established by comparing the simulation results with those of the ordinary endplate of the fuel cell data at various levels of assembly pressures. They can help determine the proper pressure and are important in obtaining a consistent fuel cell performance.

Keywords: Stack assembly; Assembly pressure; Gas diffusion layer; MEA; Pressure distribution; Compliance; FEM analysis

I. INTRODUCTION

Proton exchange membrane fuel cells (PEMFCs) are electrochemical devices that convert the chemical energy of reactants (a fuel and an oxidant) directly to electrical energy in the form of low voltage direct current (DC) electricity and heat. They have been receiving significant attention due to their high power density, energy efficiency, and environmentally friendly characteristics . However, one of the major impediments to making them a viable power source is the high manufacturing cost of a number of key components, including catalyst layers , solid polymer electrolyte (SPE) membrane , and bipolar plates .The practical operating voltage from a single cell—also known as a membrane-electrode assembly (MEA)—is about 0.7 V. Desired voltages are obtained by connecting cells in series; this is accomplished by inserting a highly conductive material (e.g., a bipolar plate) between two parallel MEAs. Such plates are by volume, weight, and cost the most critical component of a fuel cell stack , and account for more than 40% of the total stack cost and about 80% of the total weight . As a result, there have been significant R&D activities in the past few years to lower their cost, reduce their size, and improve their performance and lifetime. Bipolar plates perform a number of critical functions simultaneously in a fuel cell stack to ensure acceptable levels of power output and a long stack lifetime. They act as a current conductor between adjacent MEAs, provide pathways for reactant gases (hydrogen and oxygen or air), facilitate water and heat management throughout the stack, and provide structural support for the whole stack. Accordingly, they must exhibit excellent electrical and thermal conductivity, corrosion resistance, mechanical and chemical stability, and very low gas permeability. Furthermore, raw materials must be widely available at reasonable cost and be amenable to rapid and cost-effective fabrication methods and processes. The stacking design and cell assembly parameters in the endplate significantly affect the performance of PEM fuel cells. The dedicated integral micro-porous structures and brittle mechanical properties of the gas diffusion layer and the MEA should be preserved as much as possible after cell assembly. For example, the assembly pressure affects the characteristics of the contact interfaces between components. Insufficient assembly pressure may result in sealing problems, such as fuel leakage, internal combustion and un-acceptable contact resistance. On the other hand, too much pressure may damage the gas diffusion layer, resulting in a broken porous structure and a blockage of the gas diffusion passage. In both cases, it will decrease the cell performance, Then measured the cell performance of PEM fuel cells with different, commercially available, gas diffusion layers

Volume 4 Issue IV, April 2016
ISSN: 2321-9653
International Journal for Research in Applied Science & Engineering Technology (IJRASET)

under various assembly pressures. They found that each gas diffusion layer had its own optimal assembly pressure due to differences in mechanical properties and micro-porous characteristics. Because of the relatively thin dimensions and low mechanical strength of the gas diffusion layer and MEA versus sealant, bipolar plates and end plates, the most important goal in the stack design and assembly is to achieve a proper and uniform pressure distribution. we demonstrated that the cell performed better than the traditional nut and bolt point-load stacking design. However, there are few re-ports on the simulation of the cell assembly measurements.

A. Goals and Methodology

The goal of this research was to propose a methodology and a simulation procedure for evaluation the stacking design and cell assembly parameters. From the simulation, the methods of stacking design, the critical dimensions and material selection of fuel cell components, and assembly pressure were investigated for the purpose of achieving a consistent cell performance. The schematic plot of the methodology is shown in Fig. 1. It is composed of simulation verification . From the experimental measurement, the numerical model and the assumptions were verified for further design evaluation and parametric studies. The well-established pressure flow method was employed for the numerical simulation of the mechanical responses (stress, strain and compliance) of the cell assembly. First, the dimensions and mechanical properties of all fuel cell components were collected. the stacking sequence and components of the ordinary endplate cell in this study. The type and amount of assembly pressure depends on the type of stacking designs. In general, they can be categorized into three types: point load-design, line-load design and surface-load design. The traditional point-load design with several boltand nut assemblies . The amount of assembly pressure depends on the geometrical shape of the endplate, and on the dimensions and physical properties of all the fuel cell components. To-date it always has been determined by the trial-and-error process. Boundary conditions and the behaviour of the contacting interface of the components must be consistent with the actual physical situation. Finally, the proper types of element for each component and their interfaces must be selected so as to allow a realistic physical behaviour. Meshing is also important for an accurate result. The significant difference in thickness between the components requires special consideration in the meshing scheme. The simulated results of stress, strain, pressure distribution and the compliance contours for each component must be plotted for detailed evaluation, so that the effects of the design variables and process parameters on the cell assembly can be quantified. In order to verify the numerical model and modeling assumptions, actual experiments were conducted to measure the pressure distribution of the PEM by means of simulation, and the compliance of the gas diffusion layer for each assembly pressure. The pressure distribution was measured by means of a pressure film. The compliance was measured by COMSOl. The results were compared with those of the numerical simulation. After verification, the established numerical simulation tion procedures can be used to evaluate a new stacking design and/or optimize cell assembly parameters.

B. Analysis Process

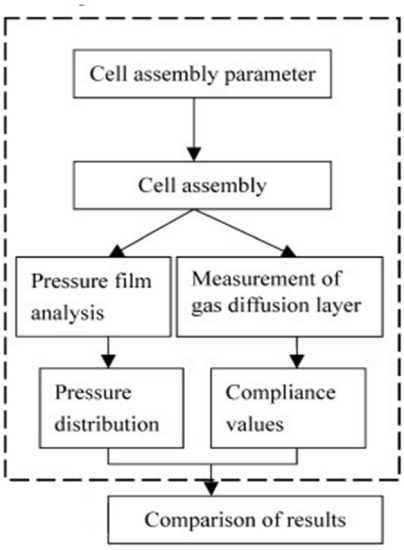

Fig. 1.

Volume 4 Issue IV, April 2016
ISSN: 2321-9653
International Journal for Research in Applied Science & Engineering Technology (IJRASET)

II. NUMERICAL SIMULATION

The PEM fuel cell is composed of several components.The contact behavior between these components is highly non-linear. A simple but effective contact model is essential for representing the actual physical phenomena with a realistic numerical model. The well-established analysis was employed for the numerical simulation. The commercial code of Pressure distribution was used in this study.

A. The PEM Model

The components of a fuel cell consist of end plates, bipolar plates, sealants, gas diffusion layers and PEM . In this study, asingle cell was designed for numerical simulation and experiments. The flow field plate integrated the functions of the endplates for mechanical strength, the current conducting platefor current collection, and the bipolar plates for flow fieldchannel, as shown in Fig. 2. The flow field plate was fabricated from Al 5052, and measured 84 mm × 84 mm × 10 mm. The flatness form error was about ±0.02 mm. The flow field channel was 1.2 mm wide by 1.0 mm deep. A polymer gasket, about 0.8 ± 0.08 mm diametre in cross-section, acted as the sealant to prevent fuel leakage. The effective fuel cell area was 50 mm × 50 mm. The gas diffusion layer was a 0.5 ± 0.03 mm thick carbon paper. It was brittle and had amicro-porous structure. The MEA was a three-layered structure with a Nafion 112 membrane, and was only 0.05 mm in thickness.. The dimensions and mechanical properties of above components are listed in Table 1. It is apparent from Table 1 that the elasticity modulus of the flow field plate, 70,000 kgf mm−2 , was much higher thanthat of the other components. The MEA had the smallest elastic modulus, 1.85 kgf mm−2 . However, it was thin and elastic and therefore may endure a certain amount of deformation. It can deform with the gas diffusion layer or the flow field plate. The gasket is elastic, and its thickness is slightly more than the gas diffusion layer. It is intended to ensure fuel sealing. It can absorb some form error as well as manufacturing tolerance of the fuel cell components. Therefore, the critical component was the gas diffusion layer due to its property of being brittle. As the gasket becomes compressed by the assembly pressure, it will accommodate the flatness error of the flow field plate as well as its own manufacturing tolerance. Then, it will compress the gas diffusion layer. If not enough pressure is applied, it may not ensure sufficient contact between the flow field plate, gas diffusion layer and the MEA. However, the brittle gas diffusion layer can be damaged if too much pressure is applied.

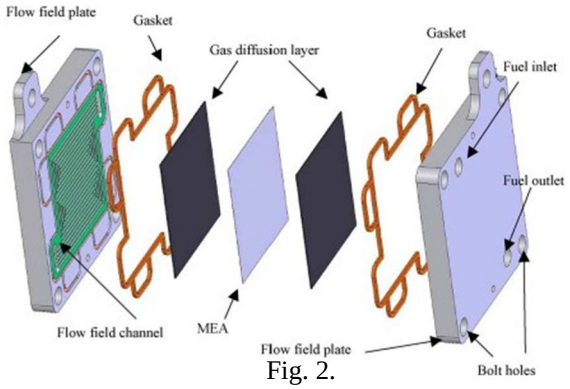

Fig. 2.

TABLE 1

Dimensions and mechanical properties of single cell components

Component	Material	Modulus of elasticity ($kgf\,mm^{-2}$)	Poisson's ratio	Size (mm)			Manufacturing tolerance (thickness) (mm)
Flow field plate	Al 5052	70000	0 .29	84	× 84	× 10	±0.02
Gas diffusion layer	Carbon paper	5.745	0.33	5	×5	× 0.5	±0.03
MEA	Nafion 112	1.85	0 .33	5	× 5	× 0.05	±0.08
Gasket	VMQ	55	0.3	φ = 0.8			

B. Flow Field Plate

Carbon is found in many compounds and is the building block of many materials. It is found free in nature in three allotropic forms: graphite, amorphous carbon, and diamond. Another type of carbon, known as buckminster fullerene, has been recently added to the

list. While diamond is one of the hardest substances known, graphite is soft and slippery. It is a crystalline form of carbon, in which each carbon atom is covalently bonded to three adjacent carbon atoms in the same plane to form six-member structures that, in turn, connect to create flat planes or sheets. The bond angle is 120° and each carbon atom uses only three of its four unpaired electrons to form strong covalent bonds with three other carbon atoms in the same plane. This arrangement creates a "free" network of electrons, where each carbon atom contributes one free (i.e., unpaired) electron to the network. One of the consequences of such an arrangement is the ability of graphite to conduct electrical current along the planes of carbon atoms, which is a highly desirable property in the manufacture of bipolar plates. However, the bond between layers is through weak van der Waals forces with larger distances, which is about 2% of the bond energy within the planes (620–720 kJ/gram atom versus 5.0–17.0 kJ/gram atom) . Consequently, graphite exhibits weak flexural strength and is more prone to fracture during fabrication than other bipolar plate materials . Nevertheless, early fuel cell research focused on graphite—natural and synthetic—as a leading material for bipolar plate construction on account of its corrosion resistance, lack of poisoning agents, and low surface contact resistance or interfacial contact resistance. However, as stated previously, graphite is brittle, permeable to gases, and exhibits poor mechanical properties. Furthermore, it is not suitable for mass production, since the fabrication of channels in the plate surfaces requires machining, a time-consuming and costly process . Additionally, after processing such as resin impregnation is often required to ensure the impermeability of graphite plates to reactant gases. Finally, the molecular structure, porosity and flexural strength of graphite have prevented a much-needed reduction in the thickness of such bipolar plates, limiting them to about 4–6 mm in thickness . This has resulted in fuel cell stacks with low power density, which is not acceptable for transportation and mobile applications. However, graphite is still considered the standard material against which most of today's bipolar plate materials are measured. The limitations as well as the advantages of graphite have led fuel cell researchers to investigate alternate materials that meet the strict requirements of high-performance, cost-effective, and durable hydrogen fuel cells.

C. Coated Metallic Bipolar Plates

A wide variety of coatings and processes have been developed to address the concerns associated with bare metallic bipolar plates. A number of common coating materials for metallic bipolar plates is presented . Such materials are often classified as carbon- and metal-based coatings. The former includes conductive polymers, graphite, diamond-like carbon and organic self-assembled monopolymers , while the latter comprises noble metals, metal carbides, and metal nitrides. Extensive research on both carbon- and metal-based coatings has been conducted and reported in the literature. It is generally agreed that such coatings must be conductive and adhere to the metallic bipolar plate substrate . Proper adhesion to the substrate is achieved by careful selection of coating materials having thermal expansion coefficients similar to those of the substrate to minimize micro- and macro crack formation. In an early report, Woodham et al. investigated the roles of thermal expansion coefficient and corrosion resistance of a number of different bipolar plates on stack performance. Wind et al. evaluated the performance of several bipolar plates, including bare 316L SS plates and plates coated with gold, in a real fuel cell environment for 100–1000 h. The amount of Fe, Ni, and Cr ion contamination in the MEAs was determined after the operation of the fuel cell. The chemical analysis of the MEAs revealed that the amount of nickel and chromium ions was substantially reduced for gold-plated bipolar plates; however, the Fe3+ content in the MEA was considerably increased compared with that of base 316L SS bipolar plates. No explanation was provided; six other coatings also were evaluated, but their chemical nature and composition were not disclosed.

D. Composites, Conductive Polymers, and Carbon-Based Coatings

Composites, conductive polymers, and carbon-based coatings offer a wide variety of possibilities. With long term viability in mind, avoiding the use of expensive metals such as silver and gold will keep the cost down. Conductive polymer coatings offer excellent corrosion resistance and can offer unique fabrication processes such as injection molding, if the entire plate is made from the polymer. By lowering the ICR of such materials, polymer bipolar plates could become the new industry standard. Carbon- based chromium coatings are reported to exhibit many favourable characteristics and should be investigated further. The incorporation of conductive metal nanoparticles into such plates is another viable option that may prove useful in lowering ICR. Fabrication of Metallic Bipolar Plates , The possibilities for fabrication of bipolar plates are very promising, as methods like stamping and hydroforming are already well established. How these processes will affect corrosion and interfacial contact resistance is, however, not well known. It has been shown that an increased stamping speed will produce a surface with a lower ICR, yet increasing the stamping force, will increase it. Further investigation into these fabrication methods is needed. The key to future fabrication of bipolar plates will be to design plates with the physical properties of metals in mind. The use of thin corrugated metal sheets, and

avoiding expensive machining processes, will lower both cost and weight of future bipolar plates.As the need for coatings on metallic bipolar plates becomes evident, many different processes are being investigated. Pack cementation of coatings onto bipolar plates is accomplished by applying a layer of the desired coating directly on the bipolar plate while heated in a furnace to high temperature. Although improvements have been observed in corrosion resistance, this process exhibits only marginal gains in ICR . This can be attributed to the formation of columnar gaps and surface defects during extended pack cementation. Greater success has been achieved by using different closed space sublimation techniques, including electron beam evaporation, physical vapour deposition, and pulsed bias arc ion plating. Although more expensive, these methods show superior performance over long-term testing. Similar to physical vapour deposition, chemical vapour deposition also deposits a microfilm layer on the substrate. In summary, metallic bipolar plates offer many advantages over traditional graphite, for example, ease of manufacturing and physical durability, however, susceptibility to corrosion and, to a lesser extent, high interfacial contact resistance have kept them from being the primary choice for the fabrication of fuel cells. In an attempt to combat this, research has been done on different corrosion resistant coatings, including, gold, silver, platinum, nickel, and several nitrides and carbides. Silver, gold, and platinum coatings are too expensive to consider for mass production, and nickel coatings do not meet the DOE requirement for ICR. Results for chromium nitride coatings have shown decreased corrosion as well, but also do not meet the DOE requirement for ICR. The most promising results have been obtained with chromium carbide coatings, with the stoichiometric ratio optimized in order to not leave excess chromium on the substrate. Different methods for depositing the corrosion resistant coatings have been researched in recent years as well, including CVD, PVD, EPD, pack cementation, ion implantation, sol-gel dip coating, and roll bonding. With cost as a major concern, most of these methods are not ideal for mass production. Future research should concentrate on a cost effective method for depositing a chromium carbide or amorphous carbon film on stainless steel plates.

E. Membrane Electrode Assemblies (MEA)

The PEM is sandwiched between two electrodes which have the catalyst embedded in them. The electrodes are electrically insulated from each other by the PEM. These two electrodes make up the anode and cathode respectively.The PEM is a fluoropolymer (PFSA) proton permeable but electrical insulator barrier. This barrier allows the transport of the protons from the anode to the cathode through the membrane but forces the electrons to travel around a conductive path to the cathode. Companies such as DuPont and Dow produce PEMs. DuPont's PEM offering can be found under the trade name Nafion. The most commonly used Nafion PEMs are Nafion XL, 112, 115, 117, and 1110.The electrodes are heat pressed onto the PEM. Commonly used materials for these electrodes are carbon cloth or carbon fiber papers.NuVant produces a carbon cloth called ELAT which maximizes gas transport to the PEM as well as moves water vapor away from the PEM. Imbedding ELAT with Noble metal catalyst allows this carbon cloth to also act as the electrode. Many other different methods and procedures also exist for the production of MEAs which are quite similar between fuel cells and electrolyzers. Platinum is one of the most commonly used catalysts, however other platinum group metals are also used. Ruthenium and platinum are often used together, if Carbon monoxide (CO) is a product of the electro-chemical reaction as CO poisons the PEM and impacts the efficiency of the fuel cell. Due to the high cost of these and other similar materials, research is being undertaken to develop catalysts that use lower cost materials as the high costs are still a hindering factor in the widespread economical acceptance of fuel cell technology. Current service life is 7,300 hours under cycling conditions, while at the same time reducing platinum group metal loading to 0.2 mg/cm2. The Membrane Electrode Assembly (MEA) is the core component of a fuel cell that helps produce the electrochemical reaction needed to separate electrons. On the anode side of the MEA, a fuel (hydrogen, methanol etc.) diffuses through the membrane and is met on the cathode end by an oxidant (oxygen or air) which bonds with the fuel and receives the electrons that were separated from the fuel. Catalysts on each side enable reactions and the membrane allows protons to pass through while keeping the gases separate. In this way cell potential is maintained and current is drawn from the cell producing electricity. A typical MEA is composed of a Polymer Electrolyte Membrane (PEM), two catalyst layers, and two Gas Diffusion Layers (GDL). A MEA with this configuration is known as a 5-Layer MEA due to its composition. An alternative version of a membrane electrode assembly is the 3-Layer MEA which is composed of a polymer electrolyte membrane with catalyst layers applied to both sides, anode and cathode. An alternative name for this type of MEA is a Catalyst Coated Membrane (CCM). See the diagram below for an example of each type:

Volume 4 Issue IV, April 2016
ISSN: 2321-9653
International Journal for Research in Applied Science & Engineering Technology (IJRASET)

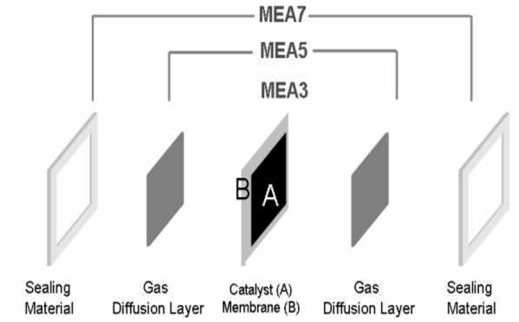

fig.3.

F. Membranes

Proton exchange membrane fuel cells, also known as polymer electrolyte membrane (PEM) fuel cells (PEMFC), are a type of fuel cell being developed for tr a nsport applications as well as for stationary fuel cell applications and portable fuel cell applications. Their distinguishing features include lower temperature/pressure ranges (50 to 100 °CTemplate:217) and a special polymer electrolyte membrane. PEMFCs operate on a similar principle to their younger sister technology PEM electrolysis.

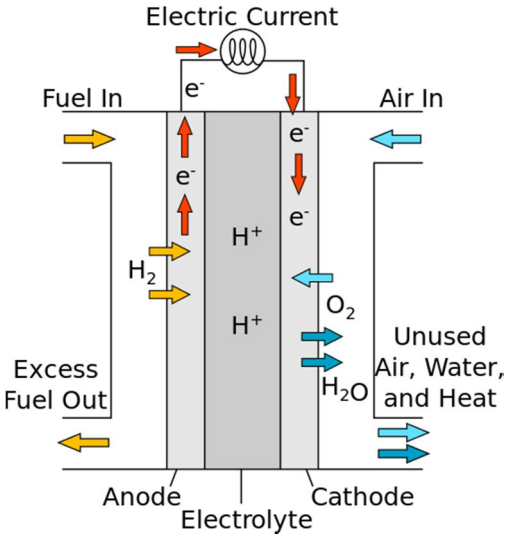

Fig.4.

They are a leading candidate to replace the aging alkaline fuel cell technology, which was used in the Space Shuttle. In order for a PEM fuel cell to operate, a Proton Exchange Membrane is needed that will carry the hydrogen ions, proton, from the anode to the cathode without passing the electrons that were removed from the hydrogen atoms. These polymer membranes that conduct proton through the membrane but are reasonably impermeable to the gases, serve as solid electrolytes (vs. liquid electrolyte) for variety of electrochemical applications, and are commonly known as Proton Exchange Membrane and/or Polymer Electrolyte Membranes (PEM). These membranes have been identified as one of the key components for various consumer related applications for fuel cells, e.g. automobiles, back-up power, portable power etc. Due to its application for many consumer markets, the technology keeps on evolving to make these membranes suitable for longer duration, and even high temperature operations.For PEM fuel cell and electrolyzer applications, a polymer electrolyte membrane is sandwiched between an anode electrode and a cathode electrode. During electrochemical reaction, oxidation reaction at the anode generates protons and electrons; reduction reaction at the cathode combines protons and electrons with oxidants to generate water. To complete the electrochemical reaction, the proton exchange membrane plays a critical role that conducts protons from anode to cathode through the membrane. The proton exchange membrane also performs as a separator for separating anode and cathode reactants in fuel cells and electrolyzers. PEMFCs are built out of membrane electrode assemblies (MEA) which include the electrodes, electrolyte, catalyst, and gas diffusion layers. An ink of catalyst, carbon, and electrode are sprayed or painted onto the solid electrolyte and carbon paper is hot pressed on either side to

protect the inside of the cell and also act as electrodes. The pivotal part of the cell is the triple phase boundary (TPB) where the electrolyte, catalyst, and reactants mix and thus where the cell reactions actually occur. Importantly, the membrane must not be electrically conductive so the half reactions do not mix. Operating temperatures above 100 °C are desireso the water by product becomes steam and water management becomes less critical in cell design.

G. Gasketing

Gaskets provide correct compression and act as a 'barrier' for potential fuel leaks; maximizing the highest possible efficiency.One of the important parameters in a fuel cell build is the thickness of the gaskets. The gasket thickness determines how much the flow fields are allowed to pinch into the electrode. For a good contact (i.e. low contact resistance), it is essential that the values are 0.002" to 0.003" for a carbon paper backing and 0.010" to 0.015" for a carbon cloth backing*. Since electrode thickness for anode and cathode may vary, gasket thickness for each side is determined separately using the formula: Gasket thickness = (individual electrode thickness) – (desired pinch)

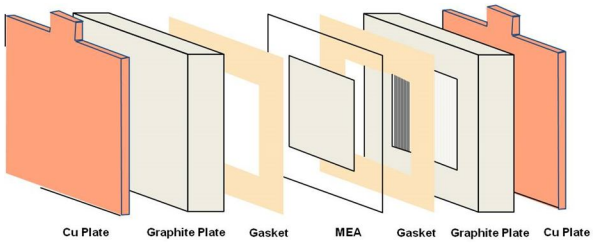

Fig.5.

These numbers are provided for guidance only. It is better to determine the pinch for individual situation with due consideration for the type of backing used and the nature of the gasket material (elastomeric materials, e.g. EPDM, tend to compress more than non-elastomeric films, e.g., PTFE)

H. Plates

Each individual MEA produces less than 1 V under typical operating conditions, but most applications require higher voltages. Therefore, multiple MEAs are usually connected in series by stacking them on top of each other to provide a usable output voltage. Each cell in the stack is sandwiched between two bipolar plates to separate it from neighboring cells. These plates, which may be made of metal, carbon, or composites, provide electrical conduction between cells, as well as providing physical strength to the stack. The surfaces of the plates typically contain a "flow field," which is a set of channels machined or stamped into the plate to allow gases to flow over the MEA. Additional channels inside each plate may be used to circulate a liquid coolant.

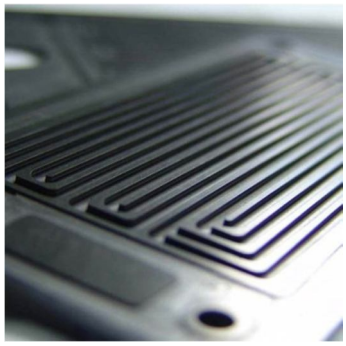

Fig.6(a)

I. Gas Diffusion Layers

The Gas Diffusion Layer (GDL) is a very important supporting material in a Membrane Electrode Assembly (MEA). Gas diffusion layers are a porous material composed of a dense array of carbon fibers, which also provides an electrically conductive pathway for current collection. GDL plays an important role of electronic connection between the bipolar plate with channel-land structure and the electrode. In addition, the GDL also performs the following essential functions: passage for reactant transport and heat/water removal, mechanical support to the membrane electrode assembly (MEA), and protection of the catalyst layer from corrosion or

Volume 4 Issue IV, April 2016
ISSN: 2321-9653
International Journal for Research in Applied Science & Engineering Technology (IJRASET)

erosion caused by flows or other factors. Physical processes in GDLs, in addition to diffusive transport, include bypass flow induced by in-plane pressure difference between neighboring channels, through-plane flow induced by mass source/sink due to electrochemical reactions, heat transfer like the heat pipe effect, two-phase flow, and electron transport. The two types of gas diffusion layers most commonly used are carbon paper and carbon cloth. Both are carbon fiber based porous materials: carbon paper is non-woven, while carbon cloth is woven fabric, thus no binder is needed.

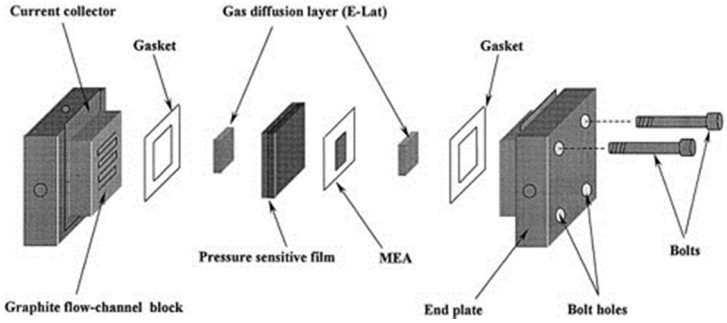

Fig.6(b)

III. SIMULATION SOFTWARE

A. *COMSOL Multiphysics*

COMSOL Multiphysics is a finite element analysis, solver and Simulation software / FEA Software package for various physics and engineering applications, especially coupled phenomena, or multiphysics. The package is cross-platform (Windows, Mac, Linux). In addition to conventional physics-based user interfaces, COMSOL Multiphysics also allows for entering coupled systems of partial differential equations (PDEs). The PDEs can be entered directly or using the so-called weak form (see finite element method for a description of weak formulation). Since version 5.0 (2014), COMSOL Multiphysics is also used for creating physics-based apps. These apps can be run with a regular COMSOL Multiphysics license but also with a COMSOL Server license. An early version (before 2005) of COMSOL Multiphysics was called FEMLAB. An application of shell and tube heat exchanger which includes the model as well; and an instance of running application.The main product is COMSOL Desktop which is an integrated user interface environment designed for cross-disciplinary product development with a unified workflow for electrical, mechanical, fluid, and chemical applications. The add-on modules blend into COMSOL Desktop, and the way of operation of the software remains the same no matter which add-on products are engaged. The Application Builder is also available with the COMSOL Desktop environment and allows for creating specialized applications, based on a physics model, with a user interface that avoids the details of the simulation model from the perspective of the end user. Two editors are available for designing applications; using drag-and-drop tools, in the Form Editor, or by programming using the Method Editor. There is scope to include specific features from the model or introduce new ones through programming using the Method Editor. COMSOL Multiphysics also provides application programming interfaces (APIs). The COMSOL API for use with Java comes included with COMSOL Multiphysics, and provides a programmatic way of driving the software through compiled object oriented code. This API is also used in the Method Editor of the Application Builder. Live Link for MATLAB allows to work with COMSOL Multiphysics in combination with the MATLAB. The Physics Builder, which is included in COMSOL Desktop, allows to create custom made physics interfaces accessible from the COMSOL Desktop with the same look-and-feel as the built-in physics interfaces. In the case of the Physics Builder, no programming is needed as it works in the COMSOL Desktop from the Physics Builder Tree, defining new user interface components. The newer Application Builder has largely replaced the Physics Builder as a tool for creating custom user interfaces for specific needs.

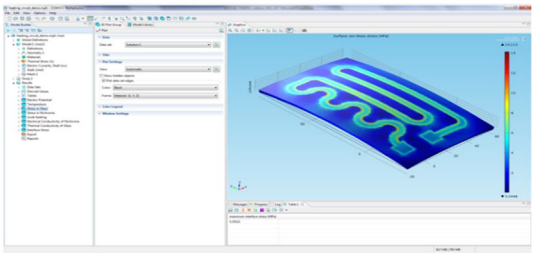

Fig.7.1.

Volume 4 Issue IV, April 2016
ISSN: 2321-9653
International Journal for Research in Applied Science & Engineering Technology (IJRASET)

A. Finite Element Model

The proper finite element type must be selected to represent the physical behaviour of each component and their interfaces. Because both the gas diffusion layer and the MEA are thin, the shell element with six degrees of freedom was selected. The 3D solid element was used to represent the flowfield plate and the gasket. In order to model the contact behaviour, the contact elements were connected between the gas diffusion layer and the MEA, the gas diffusion layer and the flowfield plate, and between the gasket and the flow field plate. A combination of mapped meshing and automatic meshing was adopted in order to ensure proper element con nectivity and a correct aspect ratio. Fig. 7.1&7.2 shows the finite element model of the single cell

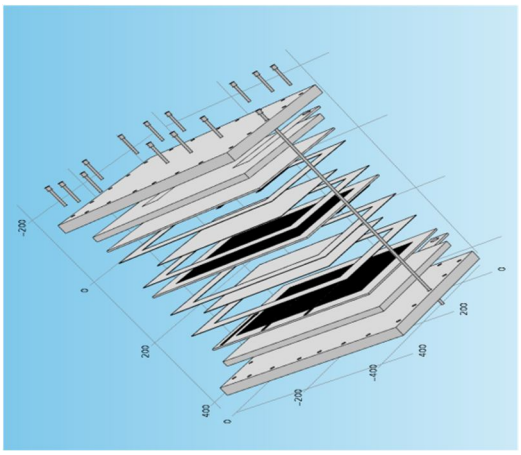

Fig.7.2(Assembly Section of the PEM fuel Cell)

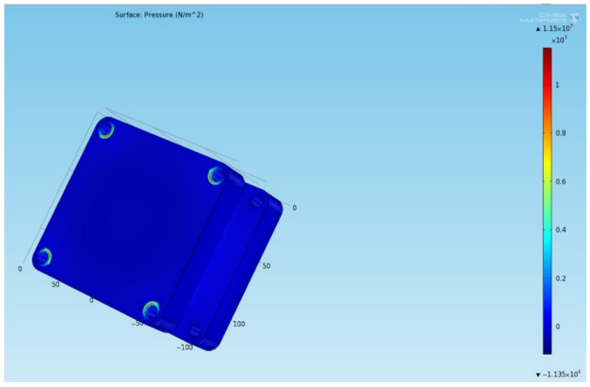

Fig.7.3.(Loading Conditions Of The finite Element Model)

B. Boundary and Loading Conditions

The assembly pressure was applied through four bolt and nut assemblies at the corners. To simplify the numerical model, the bolts and nuts were ignored in the finite element model. The assembly pressure was applied directed at the contacting areas of both flow field plates as shown in Fig.8.The finite element model had to be properly constrained in order to prevent free movement. Assuming that the model was symmetric in the middle plane, the degree of freedom of the contact elements between top and bottom gasket were assumed to be zero. This does not affect the compliance behavior of the gas diffusion layers and the gasket The results of the MEA pressure distribution and the gas diffusion layer compliance are shown in Fig. 8 andpresent the simulated pressure distribution plots of the MEA for cell assembly pressure of 15 and 25 kgf mm−2 .

These figures demonstrate that the imprint marks of the two perpendicularly oriented flow field channels are not clear when the pressure is low. However, the imprint mark becomes very clear when the assembly pressure reaches 25 kgf mm−2 . The pressure values ranged from 1.51 to 3.49 kgf mm−2 and from 1.64 to 4.21 kgf mm−2 for both cell assembly pressures of 15 and 25 kgf mm−2 , respectively. Fig. 8 also show that the pressures were higher at the four corners and lower towards the center. The simulated compliance contours of the gas diffusion layer are shown in Fig.7.1&7.2 for the assembly pressures of 15 and 25 kgf

Volume 4 Issue IV, April 2016
ISSN: 2321-9653
International Journal for Research in Applied Science & Engineering Technology (IJRASET)

mm−2 . The contours were slightly non-symmetric due the non-symmetric nature of the top and bottom flow-field plates.

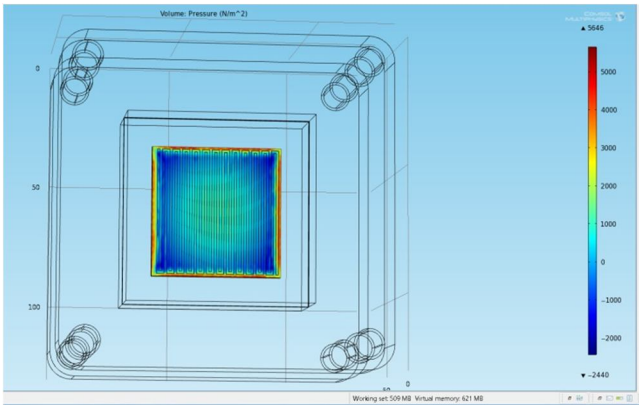

Fig.8(Pressure Distribution in the ordinary endplate)

almost zero. The contours of Fig. 8 were more definitive. Both figures show that the compliances were larger at the four corners and smaller at the center. In order to verify the effects of the point load stacking design on the pressure distribution as well as on the compliance contours, the deformation plots of the flow field plate for the assembly pressure of 25 kgf mm−2 . where clearly shows that the deformation was larger at the four corners where the pressure was applied. And then it dropped considerable toward the center creating a non-uniform distribution. This method of stack assembly is in-effective and not recommended for uniform pressure distribution. The diamond-shaped contour instead of a round contour indicates that the flow field channel had affected the strength of the flow-field plate. Fig. 8 also shows that the plate was bent. Values at nine locations of both the gas diffusion layer and the MEA, see Fig. 8, are shown for further comparison. From the contour plots, the values at locations are expected to be higher while at location the centre will be the lowest. The pressure values of the MEA at the nine locations, under the four assembly pressures, are listed in Table 1. The pressure value under the assembly pressure of 15 kgf mm−2 is about 2.1 kgf mm−2 (14%) at the four corner of locations . At the center, location 5, the pressure value is only 0.59 kgf mm−2 (4%). At 25 kgf mm−2 assembly pressure, the percentage pressure at the corner locations is about 22% and about 5% at the center. The variation in pressure distribution was large. Although the mechanical strength of the aluminum flow field plate, as shown in Table 1, was much higher than the other components, the results show that the point load stacking design is not a good method for obtaininga uniform pressure distribution at the center. This means that the center location was only touching the flow field plate. This may result in a larger contact resistance. At 25 kgf mm−2 , the compliance value at the center was about 0.032 mm, or about 6% of the original thickness of 0.5 mm. However, it was about 0.17 mm, or 34% of the original thickness, at the corners. The contact in the center may be correct, but it was reaching the limit of damaging the micro-porous structure of the gas diffusion layer. On the basis of the we have plotted a graph between the arc length as a parameter in y axis and solid as a expression in x axis . This graph represent the rate of pressure distribution in the end plate . It is calculated on the basis of rate of pressure applied the end plate of PEM fuel cell. It is calculated at the rate of pascal(pa) which is as show in the fig8.1.

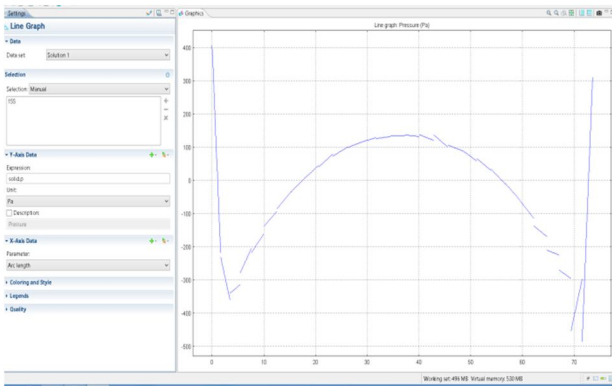

fig8.1.

In this graph the rate of pressure range is starting at above the range of 400 and then it gradually decreases to less than -300 and after it raises to above the level of 100 and then again it decreases to -300 and then it rises this is the process that has been carried out the endplate of the fuel cell.

C. Topological Optimization Design Of Endplate

A stiff structure is one that has the least possible displacement when given certain set of boundary conditions. A global measure of the displacements is the strain energy (also called compliance) of the structure under the prescribed boundary conditions. The lower the strain energy the higher the stiffness of the structure. So, the problem statement involves the objective functional of the strain energy which has to be minimized. Now the objective functional should be chosen as a function of the selection field . So in literature, people have interpolated the material properties in terms of the selection field. A widely used interpolation scheme is called the Solid Isotropic Material with Penalization (SIMP). This interpolation is essentially a power law that interpolates the Young's modulus of the material to the scalar selection field. The value of n varies between in general. This has been shown to confirm to micro-structure of the materials. So one could view topology optimization to be a process of selection of micro-structure at every point in space so that an objective functional is minimized. On a broad level, one can visualize that more the material, lesser will be the deflection as there is more material to resist the loads. So, the optimization requires an opposing constraint, the volume constraint . This is in reality a cost factor, as we would not want to spend a lot of money on the material. To obtain the total material utilized, an integration of the selection field over the volume can be done.Finally the elasticity governing differential equations are plugged in so as to get the final problem statement. ut, a straight forward implementation in the Finite Element Framework of such a problem is still infeasible owing to issues such as:

Mesh dependency—Mesh Dependency means that the design obtained on one mesh is not the one that will be obtained on another mesh. The features of the design become more intricate as the mesh gets refined.

Numerical instabilities—The selection of region in the form of a chess board.

Checker Board Patterns are shown in this result.

Some techniques such as Filtering based on Image Processing are currently being used to alleviate some of these issues.

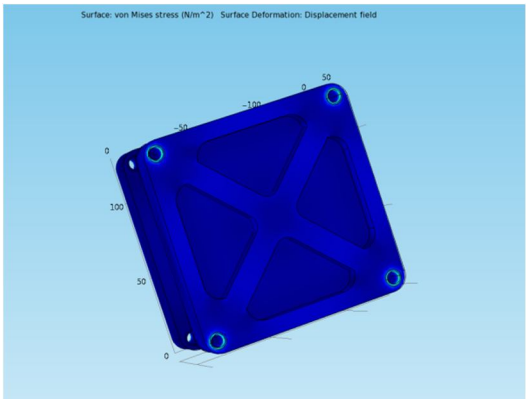

Fig 9(Topological Optimization Design Of Endplate)

the above simulation results were conducted to measure the pressure distribution of the MEA, and the compliance of the gas diffusion layer. A single cell, same as the numerical model, was built for testing, see Fig.9 . The dimensions of the cell components are listed in Table 1. The form error of the flow-field plate and the manufacturing tolerances of the other components are alsolisted in Table 1. The flatness error of the flow field plate was ±0.02 mm. The variation of gasket diameter was about ±0.01 mm. The variation in gas diffusion layer thickness was about ±0.01 mm. Measurements were taken at location of Fig. 9. Four tests with cell assembly pressures were conducted. Their values were recorded and compared with those of the numerical simulation data as presented in the below fig .9.1.

Volume 4 Issue IV, April 2016
ISSN: 2321-9653
International Journal for Research in Applied Science & Engineering Technology (IJRASET)

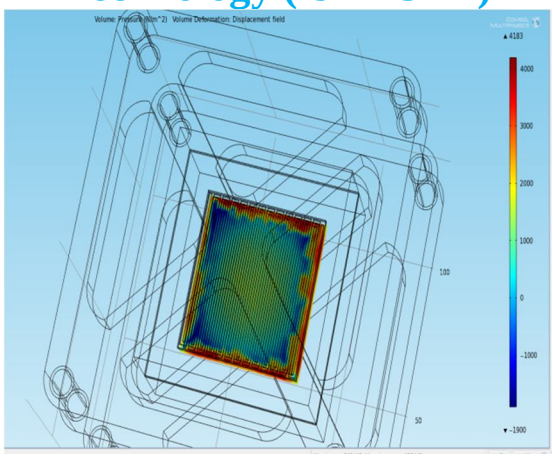

Fig.9.1

The contours of were more definitive. Both figures show that the compliances were larger at the four corners and smaller at the center on the ordinary endplate. In order to verify the effects of the point load stacking design on the pressure distribution as well as on the compliance contours, the deformation plots of the flow field plate are shown in Fig. 8.1 for the assembly pressure of25 kgf mm−2 . clearly shows that the effect of load at the center of endplate pressure difference can be seen though the colour difference was larger at the four corners where the pressure was applied. And then it dropped considerable toward the center creating a non-uniform distribution. This method of stack assembly is in-effective and not recommended for uniform mpressure distribution. The diamond-shaped contour instead of a round contour indicates that the flow field channel had affected the strength of the flow-field plate. Fig. 8 also shows that the plate pressure effect . The maximum rate of preesure will be able to obtain in the center. Values at locations of both the gas diffusion layer andthe MEA, see Fig. 8, are shown for further comparison. From the contour plots, are expected to be higher while at location 5. the center will be the lowest when it is compared to the new design . The pressure values of the MEA at the locations, under the four assembly pressures the simulated compliance values of the gas diffusion layer. At 15 kgf mm−2 , the compliance value was about to change at the corner locations and at the center. This means that the center location was only touching the flow field plate. This may result in a larger contact resistance. At 25 kgf mm−2 , the compliance value at the center was about 10% of the original thickness of has been reduced. However, it was about 0.17 mm, or 34% of the original thickness, at the corners. The contact in the center may be correct, but it was reaching the limit of damaging the micro-porous structure of the gas diffusion layer.

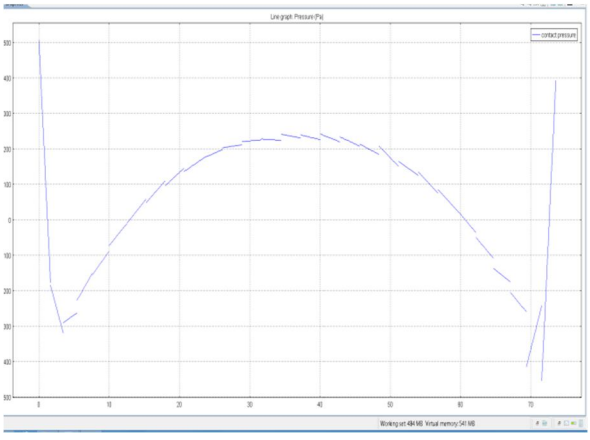

Fig.9.2

On the basis of the we have plotted a graph between the arc length as a parameter in y axis and solid as a expression in x axis . This graph represent the rate of pressure distribution in the end plate . It is calculated on the basis of rate of pressure applied the end plate of PEM fuel cell. It is calculated at the rate of pascal(pa) which is as show in the fig9.2. In this graph the rate of pressure range is starting at above the range of 500 and then it gradually decreases to less than -300 and after it raises to above the level of 200 and

then again it decreases to -400 and then it rises this is the process that has been carried out the endplate of the fuel cell.

IV. THE SIMULATION RESULTS

Fig. 9.2 and 8.1 show the measured pressure distributionof the MEA at 200 and 100Pa in the center of the cell assembly pressure .The image of Fig. 8.1 is very light meaning that the pres-sure level was low in general. The imprint mark of the flowfield channel was sparse and vague. This indicated that the MEA was not in full contact with both the gas diffusion layer and the flow field plate. The image of Fig. 9.2 was clearer with the imprint mark of the flow field channel, indicating a lower interface contact resistance. The color at the circumference was darker than in the centre. When these two measured pressure contours were compared to the simulated contours of Fig. 9.1 and 8.0, the numerical model was reasonably accurate in predicting the actual cell assembly process. Measured pressure values at nine local locations were extracted from the contours . The compliance values of the gas diffusion layer at the same locations are listed in fuel cell. The results of the trend were consistent with the numerical results of the values at the corner locations, 1, 3, 7, and 9 being larger and location 5 having the smallest value in the ordinary end plate but it is total differ in the new design of the endplate. However, they were not as denote due to manufacturing tolerances and process variations. As the assembly pressure increased, the results became more consistent Due to the Topology optimization is distinct from shape optimization since typically shape optimization methods work in a subset of allowable shapes which have fixed topological properties, such as having a fixed number of holes in them. Therefore topology optimization is used to generate concepts and shape optimization is used to fine-tune a chosen design topology.

There are various methods used to perform topology optimization:

Solid Isotropic Material with Penalisation (SIMP),

Evolutionary Structural Optimization (ESO),

Topological derivatives.

V. COMPARISON AND DISCUSSION

Data from the numerical simulation were compared with those of the experimental measurement at specific locations of Fig. 8. The percentage error was calculated by the following equation:

$$(\%)\ \text{error} = 100\% \times \frac{\text{measured value} - \text{simulated value}}{\text{simulated value}}$$

The simulated data were taken as the datum because the numerical model was ideal. There were no tolerances, variations and uncertainties. At each set of analysis variables, the simulated results will be unique and repeatable compliance were obtained for key components such as the MEA and gas diffusion layer. From these results, the effects of stack design and cell assembly procedures on stack integrity can be evaluated. A single cell of the simulated FEM model was assembled in order to record measurement data for the purpose of comparison. The percentage errors of the pressure distribution of the gas diffusion layer, and the compliance of the gas diffusion layer were within 10–60%. These errors could be caused by:

manufacturing tolerance and form error of fuel cell components.

simplified static linear model.

measurement error from pressure film color to pressure distribution contour.

However, the trends of the pressure distribution, compliance and stresses were all very similar between the measurement and the simulation. Hence, the proposed numerical simulation model and procedures could be helpful in the evaluation of stack design and cell assembly. The numerical simulation model and procedures could be extended to fuel cell stack design, to evaluate cell assembly

parameters and to specify quality control specifications, allowing for the appropriate dimensions and tolerances of the cell components to be specified. The proper combinations of fuel cell components could be evaluated in advance in order to fulfill specific functional requirements, as The values were all in the same scale. The (%) errors, in general, were larger under a smaller assembly pressure. Second, the locations of maximum and minimum values were identical for all simulated versus measured results. Third, the pressure contours from the pressure films were almost identical to those of the numerical simulated results.

VI. CONCLUSIONS

The FEM analysis method was employed to simulate the cell stack assembly of a single cell with metallic bipolar plates. The physical properties and dimensions of the fuel cell components were collected with proper boundary condition assumptions, and actual loading conditions to establish the finite element model. The contours of pressure distribution In the first stage of the cell assembly, the applied pressure was mostly to overcome the manufacturing tolerance and form errors of the fuel cell components, as listed in Table 1. As the assembly pressure increased at the new design of endplate ,then there was a stage where all the components were in elasticity deformation. After the assembly pressure exceeded the elasticity limit of some of the components, irreversible damage started to accumulate, and the characteristics of the pressure distribution and compliance became increasingly non-linear. Therefore, a cell may perform best at the second stage design of endplate of cell assembly pressure.

REFERENCES

[1] W.K. Lee, C.H. Ho, J.W.V. Zee, M. Murthy, The effects of compression and gas diffusion layers on the performance of a PEM fuel cell, J. Power Sources 84 (1999) 45–51.
[2] H.S. Chu, C. Yeh, F. Chen, Effects of porosity change of gas diffuser on performance of proton exchange membrane fuel cell, J. Power Sources 123 (2003) 1–9.
[3] D. Chu, R. Jiang, Performance of polymer electrolyte membrane fuel cell PEMFC stacks, J. Power Sources 83 (1999) 128–133.
[4] S. Giddey, F.T. Ciacchi, S.P.S. Badwal, Design, assembly and operation of polymer electrolyte membrane fuel cell stacks to 1 kW capacity, J. Power Sources 125 (2004) 155–165.
[5] R. Jiang, D. Chu, Stack design and performance of polymer electrolyte membrane fuel cells, J. Power Sources 93 (2001) 25–31.

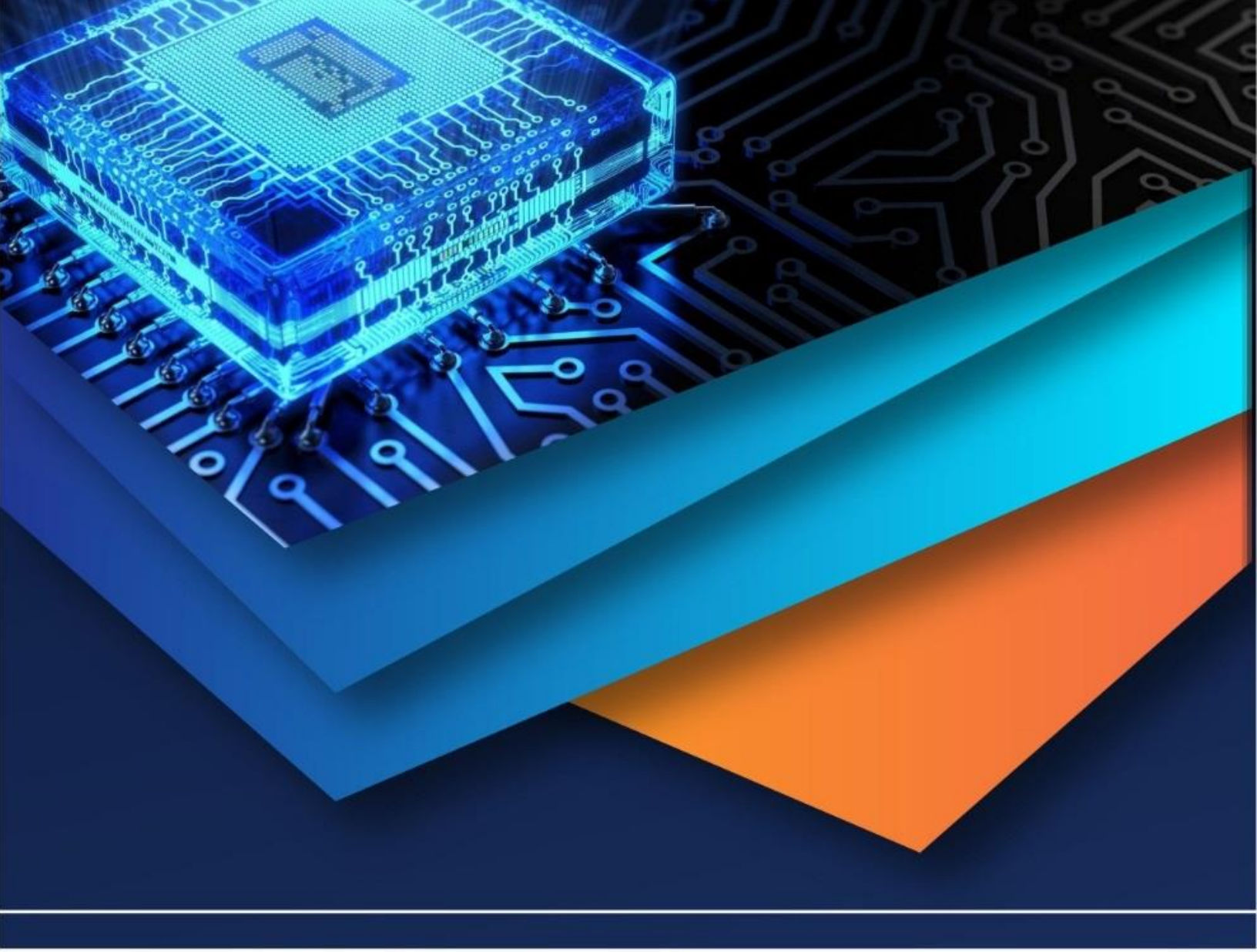

10.22214/IJRASET

45.98

IMPACT FACTOR: 7.129

IMPACT FACTOR: 7.429

INTERNATIONAL JOURNAL FOR RESEARCH

IN APPLIED SCIENCE & ENGINEERING TECHNOLOGY